New combined analysis of elastic and charge exchange $KN(\overline{K}N)$ scattering in the Regge realm

Byung-Geel Yu [*] and Kook-Jin Kong [†]
Research Institute of Basic Science, Korea Aerospace University, Goyang 10540, Korea

(Received 16 September 2019; published 13 December 2019)

The Regge features of elastic $K^{\pm}N \to K^{\pm}N$, and charge exchange $K^-p \to \overline{K}^0 n$ and $K^+n \to K^0 p$ reactions are described by using a combined analysis of all these channels at high momenta. Based on the meson exchanges in the t-channel with their decays to a $K\overline{K}$ pair allowed, the exchanges of $\rho(775) + \omega(782)$ are excluded in contrast to existing model calculations and the present paper follows a new scheme for the meson exchanges $a_0(980) + \phi(1020) + f_2(1275) + a_2(1320)$ Reggeized for the forward elastic-scattering amplitude together with Pomeron. The charge exchange reactions are described by $a_0(980) + a_2(1320)$ exchanges in the t-channel. Dominance of the isoscalar f_2 and Pomeron exchanges beyond $P_{\rm Lab} \approx 3$ GeV/c is shown in the elastic process. Both the isovector a_0 and a_2 exchanges in charge exchange reactions play the respective roles in the low- and high-momenta region. Differential and total cross sections are presented to compare with existing data. A discussion is given to the polarization of $K^-p \to K^-p$ at $P_{\rm Lab} = 10$ GeV/c and $K^-p \to \overline{K}^0 n$ at $P_{\rm Lab} = 8$ GeV/c.

DOI: 10.1103/PhysRevC.100.065206

I. INTRODUCTION

Meson-baryon scatterings are the most fundamental reactions to understand strong interaction in terms of hadronic degrees of freedom. Among these reactions, KN and $\overline{K}N$ scatterings are special because they could offer a testing ground for the formation of exotic baryons in the K^+N reaction [1–4] as well as for the kaonic bound state through the K^-N channel coupling [5,6]. In the region $P_{\rm Lab} \geqslant 3$ GeV/c, of course, the t-channel meson exchange becomes dominant and, in particular, the Pomeron exchange is expected to yield nonresonant diffraction toward high momenta up to hundreds of GeV/c in the elastic process [7].

To date, however, in comparison to an effort to understand the reaction mechanism at low momentum [6,8], attempts to describe such a high-momentum aspect of KN ($\overline{K}N$) scattering have been less challenged since after the early stage of the Regge theory where the meson exchanges were fitted to experimental data [9]. It has been a convention that the exchanges of ρ and ω mesons are included to give contributions to KN as well as a πN reaction based on the combined fitting procedure to πN and KN data with their coupling constants from the SU(3) symmetry [10–14]. On the other hand, as their decay modes to $K\overline{K}$ are forbidden kinematically, these lighter vector mesons are highly off shell and, thus, their coupling constants should also be highly model dependent if participating in the reaction. This is true for light meson exchanges in the NN scattering. In practice, the former reaction proceeds via the exchanged meson decaying to $K\overline{K}$ in the t-channel, whereas the latter case undergoes the exchange of strong force between two nucleon lines by the exchange of virtual mesons with hadron form factors. In this respect, the meson-baryon scattering could be treated differently from the baryon-baryon scattering when the exchanged mesons are required to decay to the on-shell $K\overline{K}$ pair as are the cases of ρ and ω.

Furthermore, we recall that, in the total (reaction) cross sections of $K^{\pm}p \to K^{\pm}p$ [7], the ρ and ω exchanges play a role to distinguish between K^+p and K^-p cross sections at high momenta, although far away from their on-shell propagations. However, such a conspicuous difference is not observed in experimental data between elastic $K^{\pm}p$ scatterings. Rather, they are coincident to each other in contrast to the case of the total cross section. Thus, we are led to consider a single Pomeron exchange without $\rho + \omega$ exchanges for the elastic $K^{\pm}p$ phenomena at high momenta. This issue will be pointed out in the Appendix with a demonstration of the inconsistency of the $\rho + \omega$ exchanges with the elastic $K^{\pm}p$ cross sections.

In hadron models which are based on the on-shell Born amplitudes, such as the standard pole model or its Reggeized version, it is hard to employ these lighter vector mesons without either a large uncertainty in their coupling strengths or a model dependence due to the cutoff form factors. Therefore, with a question about how the theory without $\rho + \omega$ exchanges could work on the elastic KN ($\overline{K}N$) scattering, it is worth investigating the reaction based on a new scheme of the t-channel meson exchange with those that are decaying to $K\overline{K}$ as reported in the Particle Data Group (PDG).

In our previous work [15], we investigated forward scattering of πN elastic and charge exchange processes in the Regge model where the relativistic Born terms for the t-channel

[*] bgyu@kau.ac.kr
[†] kong@kau.ac.kr

mesons were Reggeized with the interaction Lagrangians and coupling constants sharing with those widely accepted in other hadron reactions. The diffractive features of elastic reactions up to hundreds of GeV/c pion momentum were well described by the Pomeron exchange that we constructed from the quark-Pomeron coupling picture. In this paper, we extend the framework of Ref. [15] to apply for KN ($\bar{K}N$) scattering via four elastic channels,

$$K^+p \to K^+p, \tag{1}$$

$$K^-p \to K^-p, \tag{2}$$

$$K^+n \to K^+n, \tag{3}$$

$$K^-n \to K^-n, \tag{4}$$

and two charge exchange processes,

$$K^+n \to K^0p, \tag{5}$$

$$K^-p \to \bar{K}^0n, \tag{6}$$

respectively.

The paper is organized as follows. In Sec. II, we begin with the construction of the Reggeized meson exchange for elastic and charge exchange KN ($\bar{K}N$) scatterings, excluding $\rho+\omega$ exchanges as discussed in the Introduction. The t-channel meson exchanges are applied to elastic KN ($\bar{K}N$) scattering to describe the reaction at the Regge realm. Numerical consequences are compared to experimental data on total and differential cross sections at the high-momentum region. Section III is devoted to an analysis of the KN ($\bar{K}N$) charge exchange reaction to reproduce experimental data of total and differential cross sections and beam polarization asymmetry. A summary and discussion follow in Sec. IV to evaluate the physical meaning of our findings in the present approach. In the Appendix, we present numerical evidence for an elastic KN ($\bar{K}N$) cross section with and without $\rho+\omega$ exchanges to support the present approach.

II. ELASTIC KN ($\bar{K}N$) SCATTERING IN THE REGGEIZED MODEL

In the kaon elastic-scattering process on a nucleon target,

$$K^\pm(k)+N(p) \to K^\pm(q)+N(p'), \tag{7}$$

the incoming and outgoing kaon momenta are denoted by k and q and the initial and final nucleon momenta by p and p', respectively. Then, the conservation of the four-momentum requires $k+p=q+p'$, $s=(k+p)^2$, $t=(q-k)^2$, and $u=(p'-k)^2$ are invariant Mandelstam variables corresponding to each channel.

Within the present framework where the relativistic Born amplitudes are employed to be Reggeized, the exchanges of ρ and ω are discarded as discussed above. Instead, we consider vector-meson $\phi(1020)$ of $J^{PC}=1^{--}$ to assign the role generally expected from the vector-meson exchanges in the $K^\pm N \to K^\pm N$ process. Of the parity and C-parity all even, the scalar mesons $f_0(980)$, $a_0(980)$ and tensor-mesons $f_2(1270)$, $a_2(1320)$ decaying to $K\bar{K}$ are included. For the Pomeron exchange, we utilize the amplitude in Ref. [15] to describe the reaction cross sections in the momentum region $P_{\rm Lab}=100$–200 GeV/c. Therefore, we write the elastic-scattering amplitudes as

$$\mathcal{M}(K^\pm p) = f_0 + a_0 \mp \phi + f_2 + a_2 + \mathbb{P}, \tag{8}$$

$$\mathcal{M}(K^\pm n) = f_0 - a_0 \mp \phi + f_2 - a_2 + \mathbb{P}, \tag{9}$$

where the ϕ meson of C-parity odd changes sign between K^+ and K^- projectiles and the iso-vector-mesons a_0 and a_2 change signs between proton and neutron targets by isospin symmetry.

From the isospin relations between the above amplitudes,

$$\mathcal{M}(K^+n\to K^0p)=\mathcal{M}(K^+p\to K^+p)-\mathcal{M}(K^+n\to K^+n), \tag{10}$$

$$\mathcal{M}(K^-p\to \bar{K}^0n)=\mathcal{M}(K^-p\to K^-p)-\mathcal{M}(K^-n\to K^-n), \tag{11}$$

the charge exchange amplitudes are given by

$$\mathcal{M}(K^+n \to K^0p) = \mathcal{M}(K^-p \to \bar{K}^0n) = 2(a_0+a_2). \tag{12}$$

Given the Reggeized amplitudes relevant to scalar, vector, and tensor-meson exchanges in Ref. [15], we now discuss the determination of coupling constants of the meson exchange in the t-channel.

(1) Scalar meson exchange.

Scalar mesons are expected to give contributions in the low-momentum region. As to scalar meson-nucleon coupling constants, we appreciate that f_0NN and a_0NN are still hypothetical yet. From the $q\bar{q}$ structure of the scalar meson, the QCD-inspired model, such as QCD sum rules, predicts that $g_{f_0NN}=0$ and $g_{a_0NN}=12$, whereas these are $g_{f_0NN}=10.3$ and $g_{a_0NN}=-8.5$ in the case of the four-quark state $q^2\bar{q}^2$ structure [16]. On the other hand, in the vector-meson photoproduction, $\gamma p \to \phi p$, the scalar meson nonet is considered with the mixing angle θ_s between the singlet and the octet members to write the SU$_f$(3) relations among a_0, f_0, and σ mesons as [17]

$$g_{a_0NN} = \frac{F+D}{3F-D}\frac{1}{\cos\theta_s}g_{\sigma NN}, \tag{13}$$

$$g_{f_0NN} = -\tan\theta_s g_{\sigma NN}. \tag{14}$$

Given the mixing angle $\theta_s=-3.21^\circ$ and $F/D=0.575\pm 0.016$, we obtain $g_{a_0NN}=31.77\pm1.66$ and $g_{f_0NN}=0.82$ from $g_{\sigma NN}=14.6$ [18]. Therefore, within the uncertainty in the choice of $g_{\sigma NN}$, the coupling constant g_{a_0NN} is in the range of 8.5–32, regardless of its sign. We choose $g_{a_0NN}=15.5$ which is better to describe KN ($\bar{K}N$) charge exchange reactions and $g_{f_0NN}\approx 0$ which is consistent with the QCD sum rule and vector-meson photoproduction as well.

The Reggeized amplitude for the scalar meson (S) exchange employs the derivative coupling of the scalar meson to $K\bar{K}$ with the coupling vertex [15],

$$\Gamma_{SKK}(q,k) = \frac{g_{SKK}}{m_K}q\cdot k. \tag{15}$$

As the full width of the scalar meson, a_0 is in a broader range of $\Gamma(a_0)=50$–100 MeV, and no precise measurement

of the partial decay width $\Gamma(a_0 \to K\overline{K})$ is available yet, we have to estimate the partial width from PDG; $\Gamma(a_0 \to K\overline{K}) = 6.4$–$12.8$ MeV from the ratio $\Gamma(a_0 \to K\overline{K})/\Gamma(a_0 \to \eta\pi) = 0.183 \pm 0.024$ with $\Gamma(a_0 \to \eta\pi) = 35$–$70$ MeV, which is obtained by $\Gamma(a_0 \to \eta\pi)\Gamma(a_0 \to \gamma\gamma)/\Gamma(a_0) = 0.21^{+0.08}_{-0.04}$ and $\Gamma(a_0 \to \gamma\gamma) = 0.3 \pm 0.1$ keV. By isospin invariance of two decay channels K^+K^- and $K^0\overline{K}^0$, we further consider the factor of $1/2$ for the above width to get $\Gamma(a_0 \to K^+K^-) = 3.2$–$6.4$ MeV. However, because the scalar meson mass is proximity to the threshold of $K\overline{K}$ decay, the estimate of the coupling constant is highly sensitive to what mass is chosen for the $K\overline{K}$ threshold. From the decay width for the derivative coupling SKK vertex,

$$\Gamma(S \to K^+K^-) = \frac{g^2_{SKK}}{8\pi}\frac{k\left(E_K^2 + k^2\right)^2}{m_S^2 m_K^2}, \tag{16}$$

where k is three-momentum of the decaying meson in the c.m. frame and E_K is its energy, we determine $g_{a_0KK} = \pm 5.33$ with the threshold mass $m_{a_0} = 988$ and $\Gamma(a_0 \to K^+K^-) = 5.06$ MeV taken, although we use $m_{a_0} = 980$ MeV in the analysis of the reaction process.

(2) Vector-meson exchange.

The decay width $\phi \to K^+K^-$ is given by

$$\Gamma(\phi \to K^+K^-) = \frac{g^2_{\phi KK}k^3}{6\pi m_\phi^2}, \tag{17}$$

and the decay width $\Gamma(\phi \to K^+K^-) = 2.1$ MeV taken from PDG yields $g_{\phi KK} = \pm 4.46$. In ϕ vector-meson photoproduction [17,19], the tensor coupling constant $g^t_{\phi NN} \approx 0$ could obtain a consensus. However, the vector coupling constant $g^v_{\phi NN}$ is controversial; the value of $g^v_{\phi NN} = -0.24$ was used in Ref. [17] which is consistent with $g_{\phi NN} = -0.25$ by the strict Okubo-Zweig-Iizuka (OZI) rule [20]. Meanwhile, the analysis of NN and YN scatterings yields $g_{\phi NN} = \pm 1.12$ [21] and ± 3.47 [22], confirming evidence for the OZI evading process at the ϕNN vertex. From the universality of ϕ-vector-meson dominance, we here take $g^v_{\phi NN} = -3.0$ as a trial, which is close to $g_{\phi KK}$ with $g^t_{\phi NN} = 0$ for the ϕNN coupling vertex. We note that whatever values it could take among those suggested in the literature, its contribution should be insignificant in comparison to f_2 and a_2 because of the lower-lying trajectory as shown in Table I.

(3) Tensor-meson exchange.

The exchange of the tensor meson includes an isoscalar f_2 meson with the decay width $\Gamma(f_2 \to K\overline{K}) = 4.29$ MeV which is estimated from the full width 186.7 MeV with the fraction 4.6%. In the isovector channel, the a_2 meson is considered with the decay width $\Gamma(a_2 \to K\overline{K}) = 2.69$ MeV from the full width 109.8 MeV and the fraction 4.9%. The factor of $1/2$ is taken into account in both decay widths for the same reason as in the case of the scalar meson.

By using the decay width for the tensor-meson (T) coupling to $K\overline{K}$,

$$\Gamma(T \to K^+K^-) = \frac{4g^2_{TKK}}{15\pi}\frac{k^5}{m_T^4}, \tag{18}$$

TABLE I. Physical constants and Regge trajectories with the corresponding phase factors for $K^\pm N \to K^\pm N$. The symbol φ stands for a_0, ϕ, f_2, and a_2. The meson-baryon coupling constants for the vector meson and tensor meson are denoted by $g^v_{VNN}(g^t_{VNN})$ and $g^{(1)}_{TNN}(g^{(2)}_{TNN})$, respectively.

Meson	Trajectory (α_φ)	Phase factor	$g_{\varphi KK}$	$g_{\varphi NN}$
a_0	$0.7(t - m^2_{a_0})$	$(1 + e^{-i\pi\alpha_{a_0}})/2$	5.33	15.5
ϕ	$0.9t + 0.1$	$(-1 + e^{-i\pi\alpha_\phi})/2$	4.46	−3.0 (0)
f_2	$0.9t + 0.53$	$(1 + e^{-i\pi\alpha_{f_2}})/2$	3.53	6.45 (0)
a_2	$0.9t + 0.43$	$(1 + e^{-i\pi\alpha_{a_2}})/2$	−2.45	1.4 (0)

we estimate the coupling constants as $g_{f_2KK} = \pm 3.53$ and $g_{a_2KK} = \pm 2.45$ from the respective decay widths given above.

To keep consistency with the coupling constants of f_2NN in the πN scattering [15], we resume $g^{(1)}_{f_2NN} = 6.45$ and $g^{(2)}_{f_2NN} = 0$, the latter of which is rather stringent in order to agree with πN polarization observables. The determination of a_2NN coupling is discussed in the photoproduction of a charged kaon [23] where the SU(3)$_f$ symmetry dictates $g^{(1)}_{a_2NN} = 1.4$ and $g^{(2)}_{a_2NN} = 0$ to agree with experimental data. We keep these values in the present calculation.

A canonical form of the trajectory $\alpha_\varphi(t) = \alpha'_\varphi(t - m^2_\varphi) + J$ is considered for the φ Regge pole of spin J. The slopes of f_2 and a_2 are taken to be the same with those of exchange degenerate pair ω and ρ, respectively [15]. Nevertheless, the phases of f_2 and a_2 Regge poles are taken to exchange nondegenerate for the elastic process because of the absence of ω and ρ from the present calculation. The slope of the a_0 trajectory is assumed to be the same with that of scalar meson σ [15] as a member of the scalar meson nonet. The trajectory of ϕ is taken from Ref. [24]. A summary of physical constants is listed in Table I including the coupling constants and trajectories with the corresponding phase factors.

(4) Pomeron exchange.

In Ref. [15] for $\pi^\pm p$ elastic scatterings, we constructed the Pomeron exchange arising from the quark-Pomeron coupling picture.

With the Pomeron trajectory,

$$\alpha_{\mathbb{P}}(t) = 0.12\,t + 1.06, \tag{19}$$

and the quark-pion coupling strength $f_{\pi qq}$ from the Goldberger-Treiman relation at the quark level, the cross sections for $\pi^\pm N$ elastic scattering up to $P_{\rm Lab} = 250$ GeV/c were reproduced by a single exchange of Pomeron. It is straightforward to apply the formulation of the Pomeron in Ref. [15] to $K^\pm p$ elastic scattering[1] with minor changes, e.g., the quark-kaon coupling constant f_{Kqq}, the quark-Pomeron

[1]There is the Pomeron coupling to the strange quark in the KN reaction in addition to the $u(d)$ quark in the quark loop integral [15]. Nevertheless, such a difference between the two couplings by mass difference is neglected for simplicity as the quark masses between strangeness and up(down) quarks are not widely different in the constituent quarks we adopted here.

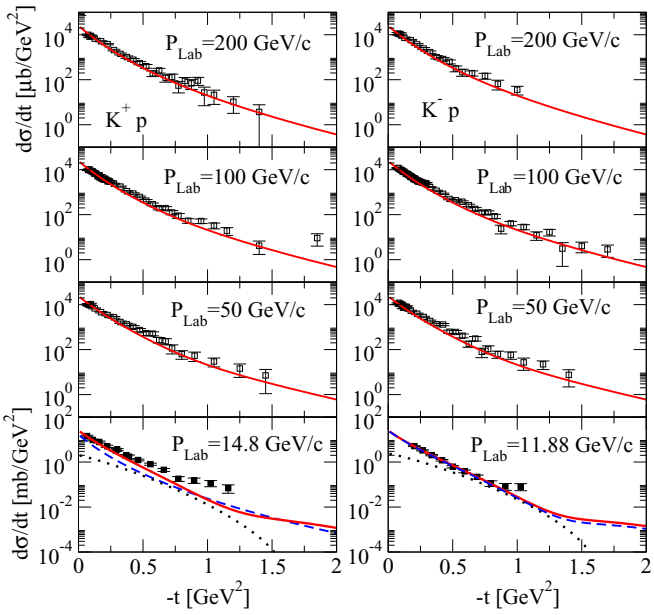

FIG. 1. Differential cross sections for elastic K^+p (left column) and K^-p (right column). Cross sections at $P_{\rm Lab} = 100$ and 200 GeV/c are featured by Pomeron exchange. Data at $P_{\rm Lab} = 50$, 100, and 200 GeV/c for both reactions are taken from Ref. [26]. Data at $P_{\rm Lab} = 14.8$ GeV/c for K^+p and 11.88 GeV/c for K^-p are from Ref. [27].

coupling strength β_s with the strange quark mass m_q, instead of those for the pion and d quark.

In numerical calculations, we take $\beta_u = 2.07$ and $\beta_s = 1.6\ \text{GeV}^{-1}$ as before [18] and $m_q = 500$ MeV in favor of the strange quark involved. Let us now determine the coupling strength f_{Kqq}. Unlike the case of $f_{\pi qq}$, however, the Goldberger-Treiman relation from the SU(3) symmetry is not likely to give a reliable answer by the large symmetry breaking. From the phenomenological point of view, the ratio of elastic cross sections for K^+p and π^+p at high momenta could be a hint to a determination of f_{Kqq} [25]. At $P_{\rm Lab} = 250$ GeV/c where there exists only the Pomeron exchange and all others are assumed to be minimal, the ratio of cross sections from world data gives

$$\frac{\sigma_{\rm el}(K^+p)}{\sigma_{\rm el}(\pi^+p)} \approx 0.836, \tag{20}$$

and, hence,

$$\frac{|\mathcal{M}_{\rm el}(K^+p)|}{|\mathcal{M}_{\rm el}(\pi^+p)|} \approx \frac{f_{Kqq}^2 m_K^2 \beta_s}{f_{\pi qq}^2 m_\pi^2 \beta_d} \approx \sqrt{0.836}, \tag{21}$$

which yields $f_{Kqq} = 0.82$ by taking $f_{\pi qq} = 2.65$ [15]. This means that, in order to obtain a better agreement with the high-momentum $K^\pm p$ data, we may well treat the quark-meson coupling constant f_{Kqq} rather as a parameter around the value above in the fitting procedure to cross-section data.

A. $K^\pm p \to K^\pm p$

Figure 1 shows the differential cross sections selected in the same momentum range to compare K^+p with K^-p elastic scatterings. Since the data at $P_{\rm Lab} = 100$ and 200 GeV/c are governed by a pure Pomeron exchange, we exploit them to determine the quark-Pomeron coupling strength and obtain $f_{Kqq} = 0.988$ with the trajectory in Eq. (19), whereas the cutoff parameter $\mu = 2.5$ GeV and $n = 1$ are fixed for the kaon form factor [15],

$$F_K(t, W) = (1 - t/\Lambda^2)^{-n}, \tag{22}$$

and $\Lambda(W) = \frac{k}{\mu}(W - W_{\rm th})$. In a good agreement with all the data selected, we regard $f_{Kqq} = 0.988$ to be reasonable because it is close to 0.82 from the ratio in Eq. (21). The dominance of the Pomeron exchange followed by the tensor-meson f_2 is shown in the lowest panels. Contributions of f_2 (dotted) and Pomeron (dashed) are shown at $P_{\rm Lab} = 14.8$ for K^+p and 11.88 GeV/c for K^-p reactions, respectively.

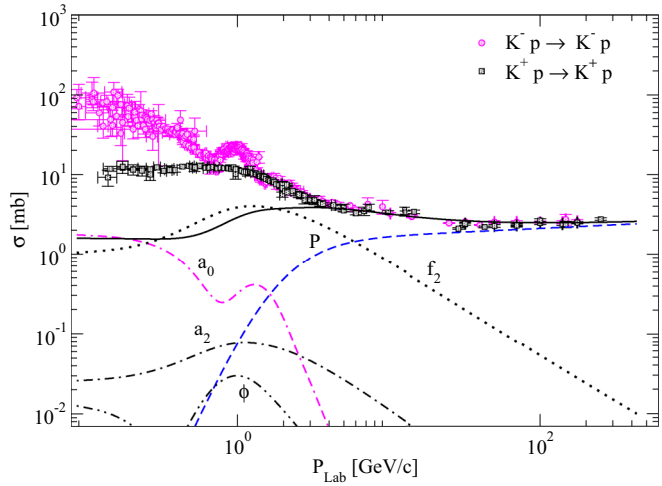

FIG. 2. Total elastic cross sections for $K^+p \to K^+p$ and $K^-p \to K^-p$. The solid curve for the total cross-section results from the full calculation of $K^+p \to K^+p$. The difference between cross sections of K^+p and K^-p is negligible by the ϕ contribution of the order of 10^{-2}. Data are taken from PDG.

In Fig. 2, we present total cross sections for K^+p and K^-p elastic processes where an agreement with data at high-momenta $P_{\rm Lab} \approx 3$ GeV/c is obtained by the exchanges of f_2 and Pomeron. Without a fitting procedure for hadron coupling constants, we describe elastic scattering over the region $P_{\rm Lab} \approx 3$ GeV/c up to 250 GeV/c. As discussed above, the distinction between the two reactions disappears at high momenta because of the small contribution of ϕ. It is worth observing the similarity between $\pi^\pm N$ [15] and $K^\pm N$ total elastic cross sections where the roles of σ, ρ, and ω in the former reactions are replaced by those of a_0, a_2, and ϕ of the same order of magnitude, respectively. Also, the $K^\pm p$ elastic scatterings are dominated by the tensor-meson f_2 at intermediate and the Pomeron exchange at high momenta to exhibit the isoscalar nature of the reactions.

Below $P_{\rm Lab} \approx 3$ GeV/c, the large discrepancy between the t-channel Regge predictions and the data could presumably

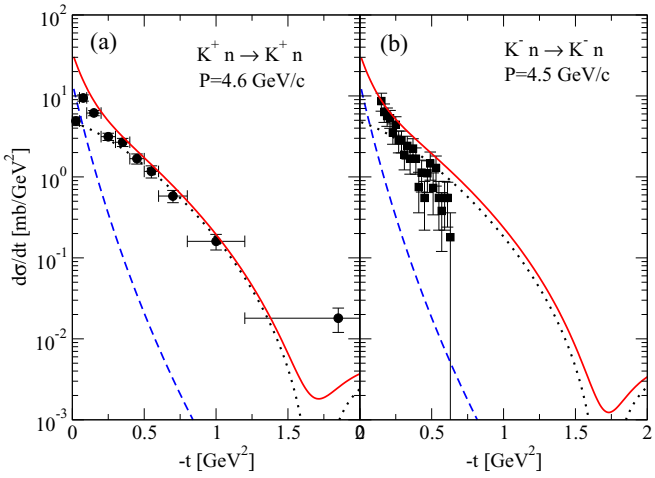

FIG. 3. Differential cross sections for $K^+n \to K^+n$ at $P_{\rm Lab} = 4.6$ GeV/c in (a) and $K^-n \to K^-n$ at $P_{\rm Lab} = 4.5$ GeV/c in (b). Notations for the curves are the same as in Fig. 2. Data are taken from Refs. [30,32], respectively.

be resolved by considering the nuclear interaction for K^+p [28] and the $\overline{K}N$ coupled states for the K^-p elastic scatterings, respectively [5].

B. $K^{\pm}n \to K^{\pm}n$

Experimental data on neutron targets are extracted from kaon scattering off a deuteron in which case the proton is assumed to be a spectator. Data at high momenta are rare and contain some uncertainties due to the procedures, such as impulse approximation, Glauber screening, and Fermi motion taken usually in the analysis of deuteron data. A few data points on the total cross section for the K^+n elastic reaction are found at $P_{\rm Lab} = 2.97$ [29] and 4.6 GeV/c [30], respectively. For the K^-n reaction, the total cross-section data are reported at $P_{\rm Lab} = 2.2$ [31] and 4.5 GeV/c [32], respectively. Therefore, no data are enough to analyze the high-momentum behavior of the reactions. Similar to $K^{\pm}p$ elastic processes, however, we expect that the difference between K^+n and K^-n elastic reactions is negligible due to the mentioned role of vector-meson ϕ. Furthermore, as the $a_0 + a_2$ exchanges in the elastic $K^{\pm}n$ reaction play the role opposite to the $K^{\pm}p$ from Eqs. (8) and (9), the difference between them could be less apparent, and the total elastic cross sections for $K^{\pm}n$ at high momentum are to be the same as those of $K^{\pm}p$ with the same role of the isoscalar exchanges f_2 and Pomeron. We present differential cross sections for K^+n at $P_{\rm Lab} = 4.6$ GeV/c and K^-n at 4.5 GeV/c in Figs. 3(a) and 3(b), respectively. We use the kaon form factor with $\mu = 2.5$ GeV and $n = 3$ for the Pomeron exchange in Eq. (22) for $K^{\pm}n$ elastic reactions. An overall agreement with the differential cross section is predicted, although the discrepancy with K^+n data in the large $-t$ is shown due to the dominance of f_2 exchange with the exchange nondegenerate phase over the Pomeron contribution in these intermediate momenta, 4.5 and 4.6 GeV/c.

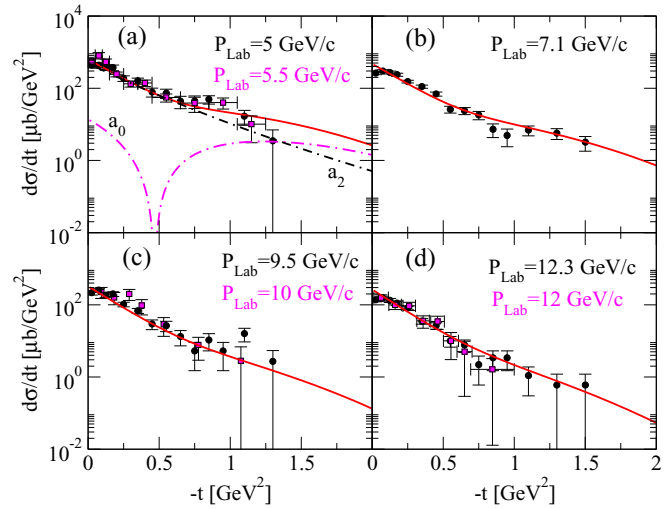

FIG. 4. Differential cross sections for $K^-p \to \overline{K}^0n$ and $K^+n \to K^0p$. The solid curves for cross sections are calculated at (a) $P_{\rm Lab} = 5.5$, (b) 7.1, (c) 10, and (d) 12 GeV/c by using the $K^+p \to K^0n$ amplitude, which shares with the $K^-p \to \overline{K}^0n$ amplitude in common. The respective contributions of $a_0(980)$ and $a_2(1320)$ are shown in panel (a). Data of $K^-p \to \overline{K}^0n$ (black circles) are taken from Ref. [33]. Data of $K^+n \to K^0p$ (magenta squares) at $P_{\rm Lab} = 5.5$, 10, and 12 GeV/c are taken from Refs. [34–36].

III. CHARGE EXCHANGE SCATTERING

Charge exchange K^+n and K^-p are good places to examine the validity of simple $a_0 + a_2$ exchanges. A collection of data on these reactions exhibits the same dependence of both cross sections upon energy and angles at high momenta as shown in Figs. 4 and 5. The differential cross sections for both reactions in the same momentum range are presented

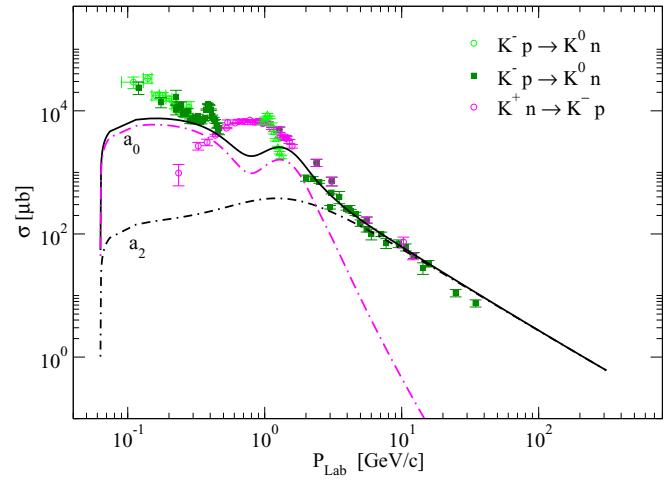

FIG. 5. Total charge exchange cross sections for $K^-p \to \overline{K}^0n$ and $K^+n \to K^0p$. The solid cross section is presented for the $K^+n \to K^0p$ process. The contribution of the a_2 exchange agrees with data at high momenta. Data of $K^+n \to K^0p$ are taken from Refs. [35,37]. Data of $K^-p \to \overline{K}^0n$ are from Refs. [30,33,38–41].

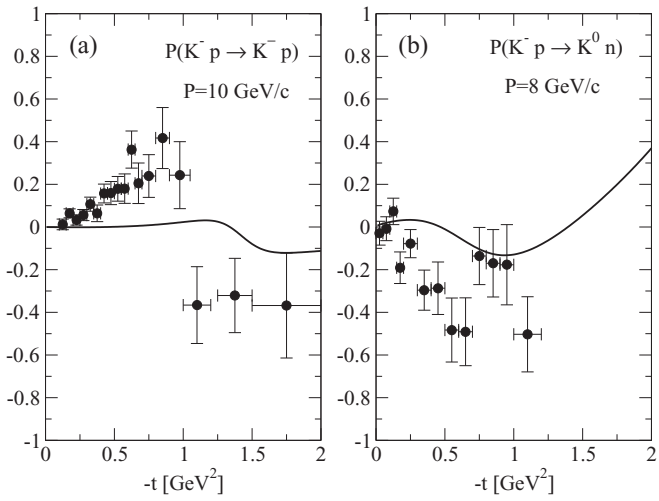

FIG. 6. Polarization P of $K^- p \to K^- p$ at $P_{\rm Lab} = 10$ GeV/c in (a) and $K^- p \to \overline{K}^0 n$ at $P_{\rm Lab} = 8$ GeV/c in (b). Data are taken from Refs. [42,43].

in Fig. 4. We obtain a fair agreement with data by using the coupling constants and the exchange nondegenerate phase for a_0 chosen in Table I for the combined analysis. However, in these reactions, the complex phase $\exp[-i\pi\alpha_{a_2}(t)]$ for the a_2 exchange is favored in order to agree with cross-section data rather than the exchange nondegenerate phase. In Fig. 5, such an expected behavior from the a_2 exchange with the complex phase is clear in the total cross section where the cross section over $P_{\rm Lab} \approx 4$ GeV/c should be reproduced only by the a_2 exchange. Meanwhile, the a_0 exchange is found to play a leading role in the low-momentum region. Throughout the successful description of reaction cross sections as presented in Figs. 4 and 5, it could be concluded that the isospin symmetry is valid among all six channels as stated in Eqs. (10) and (11).

Finally, we discuss polarization (P) of KN ($\overline{K}N$) scattering. It is observed via the interference between the spin-nonflip and the spin-flip amplitudes of exchanged mesons [15]. Therefore, we simply figure out vanishing of polarization at high momenta because there contributes only Pomeron exchange. Within the present framework, the predictions for polarization data at intermediate momenta are presented in Fig. 6. The case of $K^- p$ elastic reaction is poor as shown in panel (a). Nevertheless, due to the interference between a_0 with the exchange nondegenerate phase and a_2 with the complex phase, the polarization of $K^- p \to \overline{K}^0 n$ at $P_{\rm Lab} =$ 8 GeV/c is reproduced to some degree in panel (b). The polarization in both reactions follows the behavior of data along with the t-dependence in Fig. 6. Inclusion of the cut is likely to reinforce the strength of the polarization to agree with data as demonstrated in Ref. [15].

IV. SUMMARY AND DISCUSSION

We have performed a combined analysis of KN and $\overline{K}N$ scatterings with a set of coupling constants common in four elastic and two charge exchange processes in the Regge realm. The scattering amplitude was obtained by Reggeizing the relativistic Born amplitude for the t-channel meson exchange with the decay width to $K\overline{K}$ allowed kinematically and listed in the PDG. Thus, the exchanges of ρ and ω were excluded from the present framework, and the present approach needed none of the hadron form factors for such off-shell meson exchanges. This is the most distinctive feature from previous calculations at high momenta, although contradicting existing model descriptions.

Within the present approach, the isoscalar f_2 and Pomeron exchanges were found to be dominant in four elastic channels, whereas the charge exchange processes exhibited the isovector nature via the simple a_0 and a_2 exchanges. The exchange of the soft Pomeron which was constructed on the basis of the quark-Pomeron coupling picture reproduced the diffraction feature of elastic cross sections to a good degree. Nevertheless, in order for the present analysis to be valid for the threshold region, the inclusion of partial-wave contributions is necessary to describe the reaction mechanisms induced by either the propagation of exotic channels in K^+N reactions or the meson-baryon couplings in the $\overline{K}N$ channels. This should be a subject of future study to make complete our understanding of KN ($\overline{K}N$) scattering based on the t-channel exchange discussed here as a background contribution. Work on this direction is ongoing, and the results will appear elsewhere.

ACKNOWLEDGMENT

This work was supported by the National Research Foundation of Korea Grant No. NRF-2017R1A2B4010117.

APPENDIX: CONVENTIONAL APPROACH VERSUS THE REGGEIZED MODEL

It has been a long-standing idea that the ρ- and ω-vector-meson exchanges are included to account for the difference between $K^+ p$ and $K^- p$ total cross sections at high momenta [7]. At this point, the elastic cross section should not be confused with the total (reaction) cross section. The former reaction cross sections are observed with coincidence to each other at high momenta, which is understandable only by the isoscalar Pomeron exchange.

For illustration purpose, we make a simulation of $\rho + \omega$ exchanges, despite the decay mode neither $\rho \to K\overline{K}$ nor $\omega \to K\overline{K}$ is allowed. These vector mesons could be considered in the elastic $K^{\pm}N$ scattering by substituting $f_2 \to (f_2 \mp \omega)$ and $a_2 \to (a_2 \mp \rho)$ in Eqs. (8) and (9) [10] with the exchange degenerate phase $(a_2 \mp \rho) = 1$ or $e^{-i\pi\alpha(t)}$ for the minus or plus sign. The trajectories $\alpha_\rho(t) = 0.9t + 0.46$ and $\alpha_\omega(t) = 0.9t + 0.44$ are used. To be consistent with other meson exchanges, we avoid employing cutoff form factors in the meson-baryon coupling vertices.

However, given the coupling constants $g_{\rho KK} = g^v_{\rho NN}$ and $g_{\omega KK} = g^v_{\omega NN}$, which we usually take 2.6 and 15.6, respectively, from vector-meson dominance [12,14] the inclusion of $\rho + \omega$ exchanges lead to a complete failure in reproducing elastic data. Figure 7 shows the

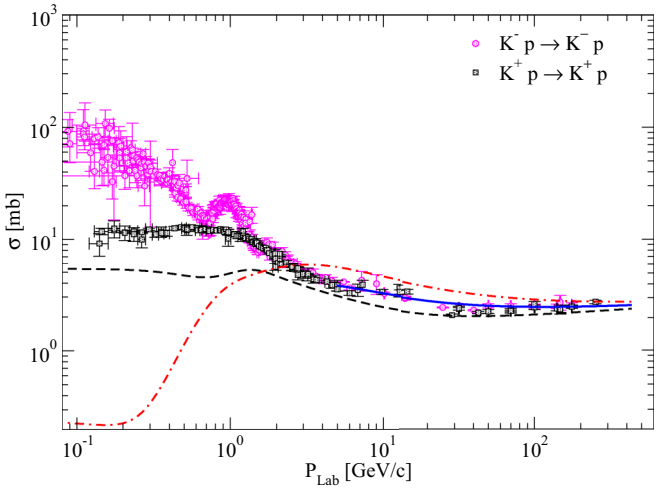

FIG. 7. Effect of $\rho + \omega$ exchanges on the elastic $K^{\pm}p$ cross sections. The discrepancy between $K^{-}p$ (upper dashed-dotted) and $K^{+}p$ (lower dashed) curves at high momenta cannot be reduced to common datasets for $K \pm p$ in the presence of $\rho + \omega$ exchanges. The solid curve from Fig. 2 is presented for comparison.

inconsistency of model predictions for the $K^{\pm}p$ elastic cross sections, even if we use such unnatural values of $g_{\rho KK} = 0.1$ and $g_{\omega KK} = -0.1$, whereas the vector-meson nucleon coupling constants remain unchanged.

As demonstrated by the solid curve for reference, the coincidence of $K^{\pm}p$ cross sections at high momenta can be achieved only from the absence of $\rho + \omega$ exchanges either or they should be negligible, at least, within the present approach. To investigate the possibility of the spin-1 vector meson further, we test the contribution of the $\rho'(1450)$ exchange with the trajectory $\alpha_{\rho'} = t - 1.23$. As the coupling constants are still evasive, we deduced $G^{v}_{\rho'} \approx 10$ and $G^{t}_{\rho'} \approx -20$ from those values of 40 and -75, which are corresponding to the πN case [15]. Assuming the universality, $g_{\rho'\pi\pi} = g^{v}_{\rho' NN} \approx 6.32$, and we take half the value of it for the present case with $g_{\rho' KK} = g^{v}_{\rho' NN}$ for the same reason. From the ratio of vector to tensor coupling, $\kappa_{\rho'\pi\pi} \approx -1.88$ is deduced. The result hardly alters the cross section in the momentum region of our interest. These findings show that they are inadequate for the present framework which is based on the nearly on-shell Born amplitude for the Reggeization of t-channel meson exchange.

[1] R. A. Arndt, I. I. Strakovsky, and R. L. Workman, Nucl. Phys. A **754**, 261 (2005).
[2] Y. I. Azimov, R. A. Arndt, I. I. Strakovsky, R. L. Workman, and K. Goeke, Eur. Phys. J. A **26**, 79 (2005).
[3] J. S. Hyslop, R. A. Arndt, L. D. Roper, and R. L. Workman, Phys. Rev. D **46**, 961 (1992).
[4] G. Giacomelli, P. Lugaresi-Serra, G. Mandrioli, A. Minguzzi-Ranzi, A. M. Rossi, F. Griffiths, A. A. Hirata, R. Jennings, B. C. Wilson, G. Ciapetti, P. Guidoni, G. Mastrantonio, A. Nappi, D. Zanello, G. Alberi, E. Castelli, P. Poropat, and M. Sessa (BGRT Collaboration), Nucl. Phys. B **56**, 346 (1973).
[5] K. Aoki and D. Jido, Prog. Theor. Exp. Phys. **2017**, 103D01 (2017).
[6] Y. Ikeda, T. Hyodo, and W. Weise, Phys. Lett. B **706**, 63 (2011).
[7] A. Donnachie and P. V. Landshoff, Phys. Lett. B **296**, 227 (1992).
[8] E. Oset and A. Ramos, Nucl. Phys. A **635**, 99 (1998).
[9] A. C. Irving and R. P. Worden, Phys. Rep. **34**, 117 (1977).
[10] R. J. N. Phillips and W. Rarita, Phys. Rev. **139**, B1336 (1965).
[11] W. Rarita and B. M. Schwamschild, Phys. Rev. **162**, 1378 (1967).
[12] R. Büttgen, K. Holinde, and J. Speth, Phys. Lett. B **163**, 305 (1985).
[13] J. Nys, A. N. H. Blin, V. Mathieu, C. Fernández-Ramírez, A. Jackura, A. Pilloni, J. Ryckebusch, A. P. Szczepaniak, and G. Fox, Phys. Rev. D **98**, 034020 (2018).
[14] F.-Q. Wu, Y.-J. Zhang, and B.-S. Zou, Chin. Phys. C **32**, 629 (2008).
[15] K.-J. Kong and B.-G. Yu, Phys. Rev. C **98**, 045207 (2018).
[16] G. Erkol, R. G. E. Timmermans, M. Oka, and T. A. Rijken, Phys. Rev. C **73**, 044009 (2006).
[17] A. I. Titov, T.-S. H. Lee, H. Toki, and O. Streltsova, Phys. Rev. C **60**, 035205 (1999).
[18] B.-G. Yu, H. Kim, and K.-J. Kong, Phys. Rev. D **95**, 014020 (2017).
[19] Y. Oh, J. Korean Phys. Soc. **43**, S20 (2003).
[20] U.-G. Meißner, V. Mull, J. Speth, and J. W. Van Orden, Phys. Lett. B **408**, 381 (1997).
[21] M. M. Nagels, T. A. Rijken, and J. J. de Swart, Phys. Rev. D **17**, 768 (1978).
[22] M. M. Nagels, T. A. Rijken, and J. J. de Swart, Phys. Rev. D **20**, 1633 (1979)
[23] B.-G. Yu, T. K. Choi, and W. Kim, Phys. Lett. B **701**, 332 (2011).
[24] P. D. B. Collins, *An Introduction to Regge Theory & High Energy Physics* (Cambridge University Press, Cambridge, UK, 1977).
[25] A. A. Godizov, Eur. Phys. J. C **76**, 361 (2016).
[26] C. W. Akerlof, R. Kotthaus, R. L. Loveless, D. I. Meyer, I. Ambats, W. T. Meyer, C. E. W. Ward, D. P. Eartly, R. A. Lundy, S. M. Pruss, D. D. Yovanovitch, and D. R. Rust, Phys. Rev. D **14**, 2864 (1976).
[27] K. J. Foley *et al.*, Phys. Rev. Lett. **11**, 503 (1963); **15**, 45 (1965).
[28] B. R. Martin, Nucl. Phys. B **94**, 413 (1975).
[29] K. Buchner, Nucl. Phys. B **44**, 110 (1972).
[30] G. Dehm *et al.*, Nucl. Phys. B **60**, 493 (1973).
[31] Y. Declais, J. Duchon, M. Louvel, J.-P. Patry, J. Seguinot, P. Baillon, C. Bricman, M. Ferro-Luzzi, J.-M. Perreau, and T. Ypsilantis, CERN-77-16, hep-database, http://cds.cern.ch/record/118289/files/CERN-77-16.pdf.
[32] C. Declercq, D. Johnson, J. Lemonne, P. Peeters, P. Renton, P. Van Binst, G. Vanhomwegen, and J. Wickens, Nucl. Phys. B **126**, 397 (1977).
[33] P. Astbury *et al.*, Phys. Lett. **23**, 396 (1966).
[34] D. Cline, J. Penn, and D. D. Reeder, Nucl. Phys. B **22**, 247 (1970).
[35] M. Haguenauer *et al.*, Phys. Lett. B **37**, 538 (1971).

[36] A. Firestone, G. Goldhaber, A. Hirata, D. Lissauer, and G. H. Trilling, Phys. Rev. Lett. **25**, 958 (1970).
[37] C. J. S. Damerell *et al.*, Nucl. Phys. B **94**, 374 (1975).
[38] T. S. Mast, M. Alston-Garnjost, R. O. Bangerter, A. S. Barbaro-Galtieri, F. T. Solmitz, and R. D. Tripp, Phys. Rev. D **14**, 13 (1976).
[39] G. S. Abrams and B. Sechi-Zorn, Phys. Rev. **139**, B454 (1965).
[40] K. J. Foley *et al.*, Phys. Rev. D **9**, 42 (1974).
[41] B. Conforto *et al.*, Nucl. Phys. B **105**, 189 (1976).
[42] M. Borghini *et al.*, Phys. Lett. B **36**, 497 (1971).
[43] W. Beusch *et al.*, Phys. Lett. B **46**, 477 (1973).